Acta Geologica Sinica (English Edition), 2020, 94(3): 707–716

Paleohydrological Changes in the Western Tibetan Plateau over the Past 16,000 years Based on Sedimentary Records of *n*-Alkanes and Grain Size

WANG Mingda[1, *], YANG Yaping[2], ZHANG Jiawu[2] and HOU Juzhi[1, 3, *]

[1] *Key Laboratory of Alpine Ecology, Institute of Tibetan Plateau Research, Chinese Academy of Sciences, Beijing 100101, China*
[2] *Key Laboratory of Western China's Environmental System (Ministry of Education), College of Earth and Environmental Sciences, Lanzhou University, Lanzhou 730000, China*
[3] *CAS Center for Excellence in Tibetan Plateau Earth Sciences, Chinese Academy of Sciences, Beijing 100101, China*

Abstract: Both monsoons and westerlies have exerted influence on climate dynamics over the Tibetan Plateau (TP) since the last deglaciation, producing complex patterns of paleohydroclimatic conditions. Diverse proxy records are essential to forge a robust understanding of the climate system on the TP. Currently, there is a general lack of understanding of the response of inland lakes over the TP to climate change, especially glacier-fed lakes. Paleohydrological reconstructions of such lakes could deepen our understanding of the history of lake systems and their relationship to regional climate variability. Here we use records of *n*-alkanes and grain size from the sediments of Bangong Co in the western TP to reconstruct paleohydrological changes over the past 16,000 years. The *P*aq record (the ratio of non-emergent aquatic macrophytes versus emergent aquatic macrophytes and terrestrial plants) is generally consistent with the variations in summer temperature and precipitation isotopes. The changes in grain-size distributions show a similar trend to *P*aq but with less pronounced fluctuations in the early-middle Holocene. The new data combined with previous results from the site demonstrate that: 1) Bangong Co experienced relatively large water-level fluctuations during the last deglaciation, with a steadily high lake-level during the early-middle Holocene and a decreasing lake-level in the late Holocene; 2) The lake level fluctuations were driven by both high summer temperatures via the melting water and monsoon precipitation. However, the dominant factor controlling lake level changed over time. The lake-level history at Bangong Co deduced from the *n*-alkanes and grain-size records reveals the past hydrological changes in the catchment area, and stimulates more discussion about the future of glacier-fed lakes under the conditions of unprecedented warming in the region.

Key words: lake level, *n*-alkane, *P*aq, grain size, Bangong Co, Tibetan Plateau

Citation: Wang et al., 2020. Paleohydrological Changes in the Western Tibetan Plateau over the Past 16,000 years Based on Sedimentary Records of *n*-Alkanes and Grain Size. Acta Geologica Sinica (English Edition), 94(3): 707–716. DOI: 10.1111/1755-6724.14538

1 Introduction

The Tibetan Plateau (TP), known as the 'Third Pole', contains the largest volumes of ice outside the polar region (Yao et al., 2018) along with thousands of lakes (Zhang et al., 2011). The dynamics of the glaciers and alpine lakes of the TP have been studied using modern monitoring data and satellite images (Yao et al., 2012; Lei et al., 2014; Yang et al., 2017). There are spatial differences in the status of the glaciers of the TP over the past decades which may be the result of changes in large-scale atmospheric circulation and temperature (Yao et al., 2012, 2018). Remote sensing and GIS techniques, together with field investigations, demonstrate that precipitation and glacial meltwater were the two most important factors influencing the lake dynamics of the region over past decades (Zhang et al., 2011; Qiao and Zhu, 2019). However, previous studies have suggested that the dominant factor controlling lake level and volume differs between periods (Qiao and Zhu, 2019). This finding necessitates the reconstruction of long-term variations in lake levels and regional climate in order to better understand the response of lake systems to ongoing climate change. Over the past decade, a greater availability of semi-quantitative precipitation isotope records (Bird et al., 2014; Günther et al., 2015), even quantitative temperature (Zhao et al., 2013; Wang et al., 2015; Hou et al., 2016; Li et al., 2017;) and precipitation records (Leipe et al., 2014; Wang YB et al., 2014) in this region, have provided opportunity to evaluate the response of paleohydrological conditions to climate changes.

The present climate of the western TP (WTP) is extremely cold and dry. Previous studies have documented the penetration of the Indian summer monsoon into the region during the Holocene (Fontes et al., 1996; Gasse et al., 1991; Gasse et al., 1996; Gasse and Van Campo, 1994;

* Corresponding author. E-mail: Dr. Mingda Wang, mdwang@itpcas.ac.cn; Dr. Juzhi Hou, houjz@itpcas.ac.cn

http://www.geojournals.cn/dzxbcn/ch/index.aspx; https://onlinelibrary.wiley.com/journal/17556724

Shi et al., 1993; Taft et al., 2020). Recent work also supports the prevalence of summer monsoon system in the WTP since the late Pleistocene (Hou et al., 2017). However, there is uncertainty about the response of the WTP lakes to climate change (Fontes et al., 1996; Kong et al., 2007). Previous studies have indicated that the lake level of Bangong Co has experienced large fluctuations (up to ~40 m) in the past in response to climatic and hydrological forcing (Shi et al., 1993; Brown et al., 2003). The results of a lake terrace study indicated that the high lake-level of the site was mainly caused by glacier melting rather than by changes in the monsoon (Kong et al., 2007). This conclusion is based on the phase relationship between the highest lake level and the timing of a decrease in monsoon intensity. Hence, this necessitates more data on what the paleohydrological regime in WTP looked like, and how the lakes respond to climate change. Is the summer monsoon the dominant factor affecting the lake's level, or is it the flow of water from nearby glaciers?

In order to better understand the long-term history of paleohydrological changes in the WTP and their response to regional climate change, we have obtained records of past hydroclimatic variability spanning the past 16,000 years from a sediment core from Bangong Co. We used *n*-alkane based *P*aq and grain-size distributions to infer lake-level changes, by combining the data with previous work on the same lake to further illustrate the hydrological conditions. Finally, we compared the Bangong Co results, in the context of records across the TP, to elucidate 1) the hydrological history of Bangong Co over the past 16,000 years; 2) the factors influencing the lake level of Bangong Co and their implications.

2 Materials and Methods

2.1 Study site

Bangong Co (33°26′ –33°58′N, 78°25′ –79°56′E, 4244 m a.s.l.) is the largest lake in the westernmost TP, with lake and catchment area of 671 km^2 and ~25,787 km^2, respectively (Khan et al., 2014; Wan et al., 2016) (Fig. 1). There is substantial spatial heterogeneity of the water quality parameters of the lake. The eastern lake basin of Bangong Co is fed mainly by meltwater from glaciers, and continuous in situ lake temperature measurements showing that it is a dimictic lake (Wang MD et al., 2014). The maximum water depth was 42.6 m, and the salinity varied little (0.47–0.55 g/L) during the summer of 2012–2017. According to NASDE (Ngari Station for Desert Environment Observation and Research, Chinese Academy of Sciences), which is ~10 km south of Bangong Co, the mean annual precipitation is 94 mm and the mean annual air temperature is 1.64°C (2010–2016). According to NASDE the modern precipitation in the region is monsoonal, with summer precipitation (JJA) accounting for more than 85% of the total (Fig. 1); this is also supported by the results of back-trajectory analysis at NASDE. At NASDE, 90% of wet deposition was transported from Nepal and northern India via the Indian monsoon (Liu YW et al., 2015). Modern precipitation isotopes monitoring in NASDE shows the isotope composition responds almost immediately to summer monsoon events, with precipitation $\delta^{18}O$ varying significantly and the large fluctuations are partly due to the summer monsoon precipitation (Wen et al., 2016). The wind rose derived from daily wind speed and direction data measured at NASDE shows southerly winds

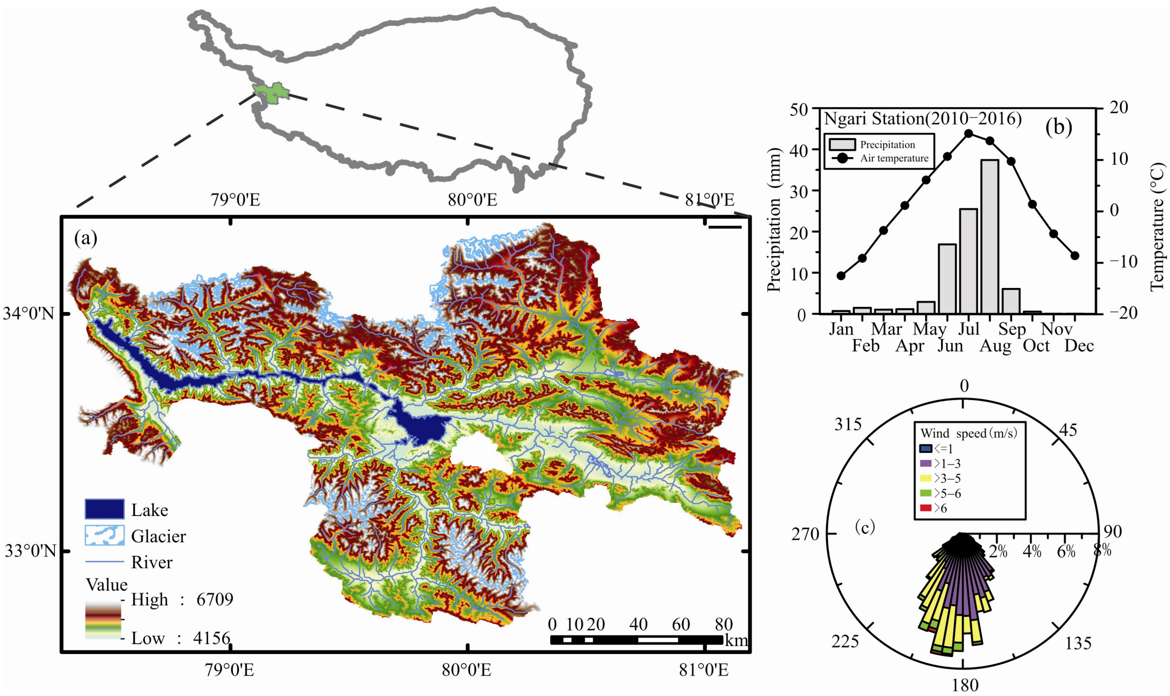

Fig. 1. (a) Map showing the catchment area of Bangong Co; (b) temporal variations of temperature and precipitation from 2010 to 2016 at NASDE (Ngari Station for Desert Environment Observation and Research); (c) wind rose showing wind speed and direction at NASDE (2011-2016, no available data for 2014).

prevailing during the summer season (Fig. 1).

2.2 Coring and dating

A 696-cm-long piston core (BGC2011-1) was collected from the southeastern part of Bangong Co in the summer of 2011 using an UWITEC platform at 20.4 m water depth. The core was subsampled at 1-cm intervals in the laboratory and then freeze-dried. The age model for the piston core is based mainly on radiocarbon dating, combined with ^{210}Pb and ^{137}Cs dating of a gravity core (BGC16-1-1G) from the same site which enabled the dating of the surficial sediments. The radionuclide activities of the 21 sediment samples from the uppermost 20.5 cm were measured with ORTEC GWL Series High-Purity Germanium (HPGe) Well Detectors. Nineteen AMS radiocarbon dates were obtained by the Beta Analytic and Peking University AMS Laboratory. The final age model for core BGC2011-1 was established using the R package *rbacon* (Blaauw and Christen, 2011).

2.3 Lipid extraction and analysis

After freeze-drying and homogenizing the sediment, a ~5 g sample was taken and subjected to ultrasonic extraction 3 times (15 min, 30° C) using a dichloromethane/methanol mixed solvent (DCM:MeOH, 2:1, v/v). The total lipid extract (TLE) was separated into neutral and acid fractions by elution through a LC-NH_2 SPE column using DCM:isopropyl alcohol (2:1, v:v) followed by ether with 4% acetic acid (v:v) as eluents. The neutral fractions were further separated into four fractions of increasing polarity by chromatography over a silica gel column using hexane, DCM, ethyl acetate:hexane (1:3, v:v) and MeOH as eluents. *n*-alkanes are contained in the first fraction (hexane) and detected and quantified using gas chromatography with a flame ionization detector (GC-FID). Samples were passed through the GC-FID (Agilent 7890A) using a HP-5 column (30 m × 0.32 mm id × 0.25 μm film thickness) for separation and then compared to an external standard (DRH-008S-R2, AccuStandard). The GC oven temperature method was as follows: initial temperature set at 60°C for 1 min, then ramp at 15 °C/min to 150°C, and then ramp at 5 °C/min to 310°C, with an isothermal hold for 20 min.

The *P*aq (non-emergent aquatic macrophyte input versus emergent aquatic macrophyte and terrestrial plant input to lake sediment) was calculated following the original equation of Ficken et al. (2000). The other well-established *n*-alkane proxy, ACL (Average Chain Length), refers to Poynter and Eglinton (1990) and Poynter et al. (1989). In the equation, Ci = peak area of *n*-alkane containing i carbon atoms. Considering the constituents of leaf waxes (Freeman and Pancost, 2014), the long-chain *n*-alkane ACL calculation was constrained from C_{27} to C_{31}.

$$Paq = (C_{23}+C_{25})/(C_{23}+C_{25}+C_{29}+C_{31})$$

$$ACL = (\Sigma[Ci]) \times i)/ \Sigma[Ci]$$

2.4 Grain-size measurements

Grain-size distributions were determined by the laser diffraction method, with a Malvern laser particle-size analyzer (Mastersizer 2000). About 0.25 g of a freeze-dried sediment sample was pretreated with 10 ml of 10% H_2O_2 to remove organic matter, then with 10 ml of 10% HCl to remove carbonates. After adding deionized water, the sample suspension was kept for 24 hours. The sample residue was then dispersed with 10 ml of 0.1 mol/L $(NaPO_3)_6$ on an ultrasonic vibrator for 5 min before grain-size analysis.

3 Results

3.1 Chronology

The sediment core recovered from Bangong Co provides a continuous sequence with a ~120-yr sample resolution spanning the past 16,000 years (Fig. 2). Chronological controls on the sediment core of BGC2011-1 from Bangong Co were constructed based on ^{210}Pb/^{137}Cs measurements from the top 20.5 cm (BGC16-1-1G, the sediment dating results are listed in Table 1) and 19 radiocarbon measurements from the deeper sediments. The $^{210}Pb_{ex}$ concentration decays exponentially with depth, and the identification of ^{137}Cs peaks corresponding to the 1963 peak in atmospheric nuclear weapons testing and the 1986 Chernobyl event agreed well with the ^{210}Pb dating results (Fig. 2). The two approaches above determine the uppermost ages of the Bangong Co sedimentary record. The radiocarbon ages of Bangong Co have been presented in Hou et al. (2017), and reservoir age (RA) is 4,833 years, as determined by linear regression of 19 radiocarbon dates. The calculated RA is different from the previous study (6,670 years) in the same lake (Fontes et al., 1996), which once again proves the spatial heterogeneity of RA at Bangong Co. Mischke et al. (2013) attributed the differences in RAs within Bangong Co to lake-atmosphere CO_2 exchange. Apparently, the RA is lower in the central part of Bangong Co since the dissolved inorganic carbon (DIC) of the lake water is presumed to be in exchange with atmospheric CO_2 for a longer time compared to other sites.

3.2 Distribution of *n*-alkanes in core BGC2011-1

In this study, the *n*-alkane composition of 140 samples has been analyzed. The sediments contained a range of *n*-

Table 1 Activities of radionuclides ^{210}Pb, ^{226}Ra and ^{137}Cs along core BGC16-1-1G

Depth (cm)	^{210}Pb (Bq/kg)	Error	^{226}Ra (Bq/kg)	Error	^{137}Cs (Bq/kg)	Error
0.5	195.5	23.3	31.8	5.3	0.0	0.0
1.5	189.0	22.7	27.3	5.3	0.0	0.0
2.5	167.0	21.9	45.0	4.8	6.7	2.6
3.5	159.9	25.2	44.0	4.9	8.1	2.5
4.5	113.1	20.8	50.6	4.8	5.1	2.6
5.5	95.6	17.9	43.4	4.1	4.7	2.5
6.5	111.0	15.6	42.2	3.9	10.9	1.6
7.5	97.8	16.1	40.8	4.0	9.0	1.9
8.5	79.5	15.9	38.2	3.9	10.1	1.5
9.5	81.9	14.4	42.1	3.7	6.6	2.0
10.5	66.4	11.2	41.4	3.1	4.4	1.6
11.5	43.0	10.4	25.5	2.5	0.0	0.0
12.5	53.5	10.0	33.7	2.8	0.0	0.0
13.5	55.2	13.2	32.6	3.4	0.0	0.0
14.5	51.9	10.9	34.2	3.1	0.0	0.0
15.5	87.0	15.3	41.0	3.8	0.0	0.0
16.5	47.4	14.0	37.9	3.5	0.0	0.0
17.5	50.6	12.0	34.1	3.4	0.0	0.0
18.5	67.1	12.5	39.8	3.1	0.0	0.0
19.5	42.3	12.9	36.9	3.1	0.0	0.0
20.5	45.4	10.1	41.2	3.1	0.0	0.0

alkanes from C_{15} to C_{31}. Based on the *n*-alkane distribution, the profiles of *P*aq and ACL were divided into three distinct periods (Fig. 3). Period I, the last deglaciation (here referred to 16–12 cal kyr BP), is characterized by middle-chain *n*-alkanes, and the *P*aq values are the highest, varying between 0.60-0.96. Increasing trends are observed for both $ACL_{27\text{-}31}$ and $ACL_{21\text{–}31}$, while significant changes appear around 13 cal kyr BP; in Period II, early–middle Holocene (12–4.7 cal kyr BP), the contributions of long-chain *n*-alkanes increases gradually, *P*aq values are relatively low, fluctuating between 0.29 and 0.64 with an average of 0.45. The variations of $ACL_{27\text{-}31}$ are small, showing a slight upward trend. The $ACL_{21\text{–}31}$ reaches a plateau between 8.2–6.6 cal kyr BP; in Period III, late Holocene (4.7 cal kyr BP to the present), *P*aq increased overall, from 0.45 to 0.85, and $ACL_{21\text{-}31}$ showed a similar trend. $ACL_{27\text{–}31}$ exhibited obvious fluctuations with significant decreases at ~1 and ~2.3 cal kyr BP.

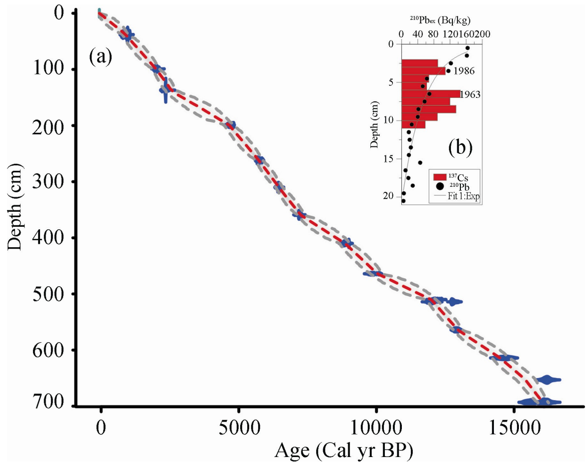

Fig. 2. (a) Age-depth model for sediment core BGC2011-1. The model was constructed using the R package *rbacon*. (b) Age-depth model based on the ^{210}Pb and ^{137}Cs chronology of the surficial sediments in core BGC16-1-1G.

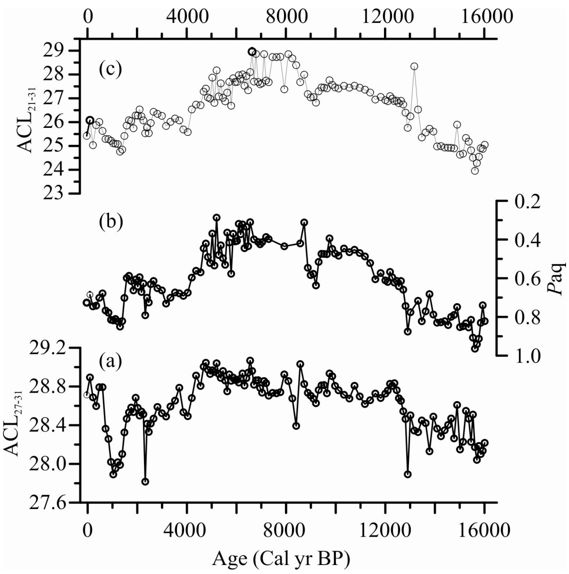

Fig. 3. Records of *n*-alkane proxies from core BGC2011-1.
(a) $ACL_{27\text{-}31}$, (b) *P*aq, (C) $ACL_{21\text{-}31}$.

3.3 Sediment grain-size distributions in core BGC2011-1

The grain-size distributions of 269 samples was analyzed and the results are illustrated in Fig. 4. The temporal trends in grain-size distributions can also be divided into the three periods described above. During the last deglaciation (16–12 cal kyr BP), there were large variations in grain size with the mean grain size ranging between 11 and 80 μm. The ranges of contents of sand (> 64 μm) and fine-medium silt (2–16 μm) are 3–40% and 28–66%, respectively. During the early-middle Holocene (12–4.4 cal kyr BP), the grain size was relatively uniform and the sand content fluctuated between 1% and 11%. In the late Holocene (from 4.4 cal kyr BP to the present), the sand content varied from 2% to 25%, and the mean grain size consequently increasing gradually from 13 to 49 μm.

4 Discussion

4.1 Proxy interpretations

4.1.1 *n*-alkane proxies

Sources of *n*-alkanes

Understanding the sources of *n*-alkanes is vital for the interpretations of sedimentary *n*-alkane records. Mid-chain *n*-alkanes (e.g. C_{23} and C_{25}) are primarily produced by non-emergent macrophytes (submerged and floating plants) and long-chain *n*-alkanes (e.g. C_{29} and C_{31}) are mainly derived from terrestrial higher plants (Diefendorf and Freimuth, 2017; Ficken et al., 2000; Gao et al., 2011). The *n*-alkane distribution of modern plants across the TP is consistent with previously reported cases (Duan and Xu, 2012; Guenther et al., 2013; Mügler et al., 2008; Witt et al., 2016). However, recent work on the TP suggests that submerged plants may also potentially contribute significantly to the sedimentary C_{27} and C_{29} pool (Aichner et al., 2010; Liu and Liu, 2016; Liu WG et al., 2015). Although there is no *n*-alkane distribution in modern

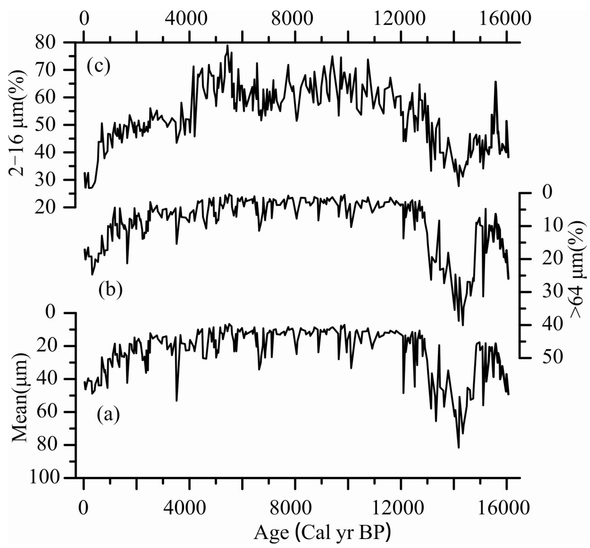

Fig. 4. Grain-size records from core BGC2011-1.
(a) Mean grain size, (b) Sand fraction content (> 64 μm), (c) silt fraction content (very fine to medium silt, 2–16 μm).

plants reported in the current study, the modern terrestrial higher plants and aquatic plants in the catchment of Bangong Co were investigated by Hu et al. (2014). They found that C_{23} was predominantly derived from aquatic plants and C_{27}–C_{33} from land plants, although the perennial herb *Potentilla anserine* and a woody plant *Salix* sp. with a dominant *n*-C_{25} peak have been reported.

Interpretations of *P*aq and ACL

*P*aq is useful for evaluating the contribution of *n*-alkanes from non-emergent aquatic plants relative to emergent and terrestrial plants, which could be associated with fluctuations in the lake levels and climatic conditions (Callegaro et al., 2018; Liu et al., 2017; Sun et al., 2018; Wang et al., 2019). Currently, there are two opposite interpretations of *P*aq as an indicator of water depth: high *P*aq can be interpreted to indicate either decreasing lake level (Liu et al., 2017; Sun et al., 2018; Wang et al., 2016; Wang et al., 2020) or increasing lake level (Callegaro et al., 2018; Chu et al., 2014; Pu et al., 2011; Wang et al., 2017; Zhang et al., 2017). To better understand this paradox, we reexamined the calculation of *P*aq. *P*aq can be simplified to the ratio of submerged to terrestrial plants due to the relatively small amounts of floating and emergent plants across the TP. Hence, the changes in *P*aq are mainly controlled by the relative proportions of submerged plants and terrestrial plants. There is a consensus on the impact of climate on lake level and land plants. A high lake level associated with wet, warm conditions would benefit land plant growth. However, there are different understandings of the growth of submerged macrophytes under varying water levels, the significant input from submerged plants either being interpreted as the response to lake shrinkage (Liu et al., 2017; Sun et al., 2018) or expansion (Callegaro et al., 2018; Wang et al., 2017; Zhang et al., 2017). Previous studies indicated that the growth of submerged plants depends mostly on the morphometric characteristics of the littoral zone and the water transparency (Duarte and Kalff, 1986; Middelboe and Markager, 1997). Hence, the distribution of submerged biomass responding to changes in lake level varies among lakes. For Bangong Co, *P*aq varies between 0.29 to 0.96 over the past 16,000 years, and indicates a large biomass of submerged macrophytes in the lake. The lake level of Bangong Co was assumed to be 30–35 m higher between 8.5–8.3 kyr BP (uncalibrated ages) than today (Shi et al., 1993). Hence, the submerged plants may be constrained by light attenuation in the water column if the water level remains high (Middelboe and Markager, 1997). In this study, we used *P*aq to infer lake-level history, with lower *P*aq indicating a higher water level associated with more terrestrial plants and less submerged macrophytes, and vice versa.

We also calculated the *n*-alkane ACL over different chain length ranges. Freeman and Pancost (2014) highlighted the necessity of defining ACL with the molecular range in subscripts to avoid confusion. Hence, it is important to carefully select the carbon numbers for the ACL calculations. Here we calculated the ACL using two different carbon ranges, $ACL_{27\text{-}31}$ (long-chain *n*-alkane ACL) and $ACL_{21\text{-}31}$ (mid-chain and long-chain *n*-alkane ACL). The ACL of long-chain *n*-alkanes in sediments potentially reflects climate changes (Pu et al., 2013; Zhang et al., 2017), while $ACL_{21\text{-}31}$ reflects the sources of organic matter (Günther et al., 2016; Jin et al., 2015; Saini et al., 2017; Witt et al., 2016).

Although many previous surveys aimed to clarify the climate determinants of plant wax *n*-alkane ACL, there is still no consensus regarding the dominant factor. ACL is reported to respond to aridity (Eley and Hren, 2018; Schefuß et al., 2003) and/or temperature (Bush and McInerney, 2015; Wang et al., 2018). In general, ACL increases with higher temperatures and/or drier conditions. For the lakes in the TP, the long-chain *n*-alkane ACL is either interpreted in terms of temperature (Ling et al., 2017a; Pu et al., 2013; Pu et al., 2011) or relative humidity (Ling et al., 2017b; Zhang et al., 2017). There have been many approaches to ACL calibration across the TP (Bai et al., 2019; Guo et al., 2015; Jia et al., 2016) and modern calibrations based on lake sediments (Hu et al., 2014; Ling et al., in press). For example, Hu et al. (2014) showed that the ACL changed in response to precipitation, increasing in wetter conditions. In the present study, we speculate that the long-chain alkane ACL responds to precipitation variations, but further evidence is needed to clarify the impact of climatic variables on long-chain ACL for the lakes of the TP. In addition, $ACL_{21\text{-}31}$ has been used to characterize organic matter sources in sediment (Callegaro et al., 2018; Günther et al., 2016; Saini et al., 2017; Yan et al., 2020).

4.1.2 Interpretation of grain-size variations

The grain-size distributions of lake sediments are an important indicator of sediment sorting processes, that can be used to reconstruct hydroclimatic variability (Dietze et al., 2014; Macumber et al., 2018; Peng et al., 2005). However, the environmental factors controlling grain-size variations may vary on different timescales (Chen et al., 2004), including runoff associated with rainfall (Peng et al., 2005) and lake level variations (Wünnemann et al., 2006). For long timescales, e.g. the centennial scale, coarsening trends in lake sediment records can reflect a lowering of the lake water level and the increased proximity of the core site to the shoreline (Macumber et al., 2018). Since Bangong Co has experienced large lake-level fluctuations during the late Pleistocene (Shi et al., 1993; Shi et al., 2001), we interpret a decrease in grain size to indicate an increase in lake level.

4.2 Lake level reconstruction for Bangong Co

The *P*aq interpretations outlined above highlight the importance of using multiple proxies to reconstruct paleohydrological changes, because a single proxy record can sometimes be interpreted in two opposite ways (He et al., 2014). We used *P*aq and grain-size distributions from the same sediment core to infer the lake-level changes. Furthermore, we explored the changes in paleohydrological conditions of Bangong Co during the Holocene by combining the new results with previous records from the same lake obtained using other proxies, such as diatom assemblages (Fan et al., 1996) and the $\delta^{18}O$ of authigenic carbonates (Fontes et al., 1996). Both the biomarker record and the grain-size record showed that the lake level experienced obvious fluctuations over the past 16,000 years. The new records are concordant with previous studies in Bangong Co over the Holocene, inferred from multi-proxy studies of lake sediment (Fan et al., 1996; Fontes et al., 1996). The inferred lake level history could be subdivided into three periods (Fig. 5), which are described below.

Period I (16–12 cal kyr BP): The lake level history recorded by *P*aq depicts a gradual expansion of Bangong Co during this period. However, the grain-size distributions reveal significant changes in the hydrodynamics of the lake basin (Fig. 4). The inconsistency between the proxy records during this period may be due to differences in the response of the biological and physical proxies. For example, the variations in the *P*aq index slightly precede those of grain size (Fig. 5). It is possible that there are differences in the timing of the response of plants compared to transport and deposition process revealed by grain size record. Biomarker proxies may be more sensitive to lake level changes than grain-size distributions in some cases. Bangong Co was relatively shallow during the last deglaciation, and the rapid changes in grain size are reasonable since slight changes in temperature and water supply would result in the larger response of a shallow lake under glacial conditions (Witt et al., 2016). In contrast, the unfavorable environment, with low precipitation and cold soil condition, may have constrained the development of terrestrial ecosystems, resulting in the relatively low variability of *P*aq. At 13 kyr BP, there was a sharp increase in *P*aq, indicating declining lake levels; this is supported by other evidence, such as the isotopic composition of authigenic carbonate (Fontes et al., 1996) and the percentages of saline water diatom species (Fan et al., 1996).

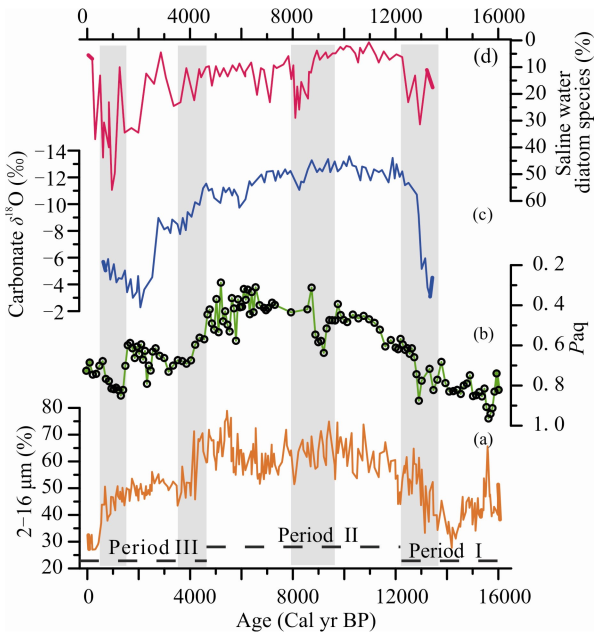

Fig. 5. Reconstructions of the paleohydrological condition at Bangong Co.

Comparison of *P*aq and grain-size records of core BGC2011-1 with published records from the same lake. (a) Silt fraction (2–16 μm) (this study), (b) *P*aq record (this study), (c) Bangong Co δ^{18}O of authigenic carbonate (Fontes et al., 1996) with a revised chronology, (d) Percentages of saline water diatoms (%) (Fan et al., 1996) with a revised chronology. The shaded area indicates shallow water conditions.

Period II (12–4.7 cal kyr BP): Evidence for lake level changes from multi-proxy records reveals that a deep-water environment occurred during the early-middle Holocene. The water level decreased substantially at ~8–9 kyr BP (Fig. 5), lasting for ~1,000 years, supported by the lake precipitation/evaporation ratio (P/E) history, as revealed by calcite δ^{18}O and the evidence of diatom species (Fan et al., 1996). The percentages of saline diatom species (living in oligosaline and mesosaline waters) sharply increased from 4% to 29%, indicating that the water became more saline, as a result of lake shrinkage.

Period III (4.7 cal kyr BP to the present): The water level gradually decreased in the late Holocene, indicating a pronounced shrinkage of the lake, despite a slightly higher level between 2.7 and 1.6 kyr BP (Fig. 5). The lake reached its lowest level at ~1 kyr BP.

4.3 Paleohydrological response to climate change in Bangong Co

The gradual expansion of Bangong Co between 16 and 12 cal kyr BP was probably due to the increase in both rainfall and ice melting. After 14 kyr BP, both *P*aq and the grain-size record indicate a rising trend of the lake level under more favorable climatic conditions. Climatic oscillations occurred and wet/dry spells were distinctly recorded by leaf wax δD records in the catchment (Hou et al., 2017). A cold climate would have had a greater influence on terrestrial plants than on submerged aquatic plants (Lin et al., 2008), resulting in high *P*aq values. The inferred lake shrinkage at ~9 kyr BP was coincident with a decrease in summer temperature at the same time (Hou et al., 2016; Zhao et al., 2017). We speculate that the low water level was mainly caused by the reduced snow and ice melting due to the cold event. The leaf wax isotope record indicated that humid conditions prevailed, with negative isotope values and only minor fluctuations, indicating that the impact of monsoon precipitation on the water level was limited. The reconstructed lake level variations in the late Holocene are generally consistent with previous climatic records (Fig. 6). The *P*aq-inferred lake level covaried with both summer temperature and precipitation isotope variations, demonstrating a pronounced lake response to climate changes. The lake was becoming shallower due to the climatic deterioration, with less precipitation and variations in temperature.

Our reconstructed lake-level history reveals that both meltwater and monsoon precipitation have contributed to lake expansion and shrinkage over the past 16,000 years. High temperatures resulted in accelerated glacier melting which increased the lake level. Pu et al. (2011) found a similar trend between *P*aq and temperature at an alpine lake in the eastern TP. It is to be noted that the inferred lake level differs from two records of mean annual air temperature, based on isotope variations in the Guliya ice core (Thompson et al., 1997) and the GDGT temperature record from a saline lake in the WTP (Li et al., 2017) (Fig. 6). It is beyond the scope of the present study to explore

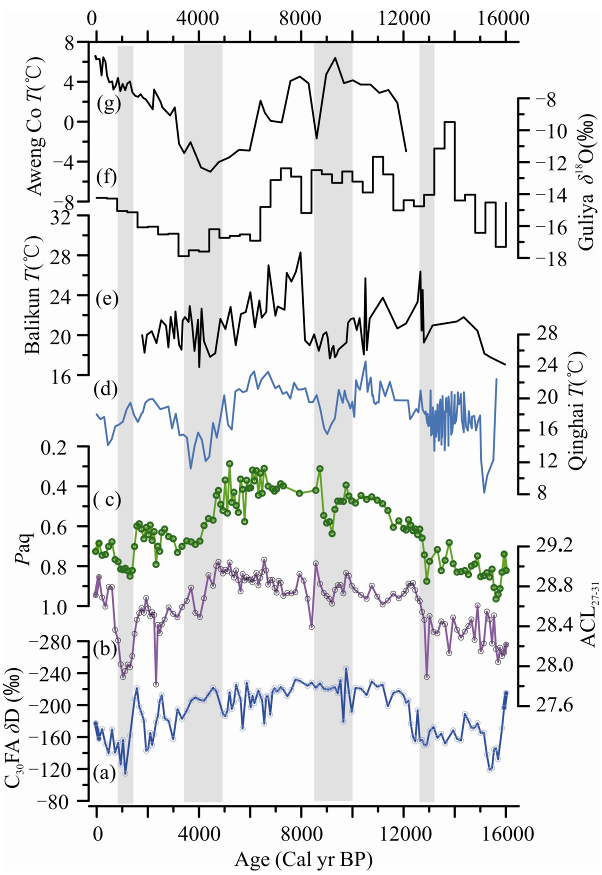

Fig. 6. Comparison of the paleoenvironmental records from Bangong Co with regional paleoclimatic records.
(a) δD of n-C_{30} acids of core BGC2011-1 (Hou et al., 2017), (b) Long-chain n-alkane ACL record of core BGC2011-1 (this study), (c) Paq of BGC2011-1 (this study), (d) Alkenone-inferred temperature reconstruction from Lake Qinghai (Hou et al., 2016), (e) Alkenone-inferred temperature reconstruction from Lake Balikun (Zhao et al., 2017), (f) Guliya ice core δ^{18}O record (Thompson et al., 1997), (g) GDGT-inferred temperature record from Aweng Co (Li et al., 2017). The shaded area indicates shallow water conditions.

the reasons for the discrepancy between the mean annual and summer temperature records. However, it is possible that most of the meltwater was delivered during the summer season, which is supported by temperature data from NASDE and modern in situ monitoring. Weather station data indicate that the monthly average air temperature is around or below zero for more than six months of the year (Fig. 1), and the monitoring results show that the lake is ice-covered from November to April (Wang MD et al., 2014).

The δD of sedimentary leaf waxes can be used as a proxy for precipitation δD variations (Hou et al., 2008; Sachse et al., 2012), even in very dry regions such as the TP (Hou et al., 2018). In this study, we used the δD of C_{30} n-acid (hereafter δD_{wax}) from the same sediment core to reconstruct precipitation D/H ratios. The long-term δD_{wax} values over the past 16,000 years are interpreted to reflect past changes in effective precipitation as well as summer monsoon intensity, which have been discussed previously (Hou et al., 2017). More depleted isotopes are attributed to a moister climate, potentially resulting in a rising lake level and decreased Paq values, and vice versa. The lake level generally paralleled the precipitation isotope curve, despite the absence of obvious change in precipitation during intervals of low lake level, such as the high Paq at ~9 kyr BP.

5 Conclusions

The new biomarker-based and grain-size records from Bangong Co provide new insights into the lake-level history in the WTP. Bangong Co experienced relatively large lake-level fluctuations during the last deglaciation, a sustained high lake level during the early-middle Holocene and a decreasing lake level in the late Holocene. The lake-level fluctuations were driven by both summer temperature via meltwater, and monsoon precipitation. However, the dominant factor controlling lake level differs between periods. In subsequent research it is important to focus on quantifying changes in lake volume and to estimate the respective contributions of meltwater and precipitation.

Acknowledgments

We thank Mr. Wenjing Zhang, Dr. Yue He and Mr. Li Lei for their assistance in the field and Mr. Shaopeng Gao from the Key Laboratory of Tibetan Environment Changes and Land Surface Processes, ITPCAS, who conducted the ^{210}Pb/^{137}Cs analyses. We also thank Dr. Asif Khan for providing the shape files of the Bangong Co catchment area and Dr. Junbo Wang for the bathymetric data of Bangong Co. We thank the editors and reviewers for their helpful comments and Jan Bloemendal for English improvement. This research was financially supported by the Natural Science Foundation of China (41601205, 41772178, 41072120).

Manuscript received Mar. 1, 2020
accepted Apr. 2, 2020
associate EIC: CHEN Fahu
edited by Jeff LISTON and FEI Hongcai

References

Aichner, B., Herzschuh, U., and Wilkes, H., 2010. Influence of aquatic macrophytes on the stable carbon isotopic signatures of sedimentary organic matter in lakes on the Tibetan Plateau. Organic Geochemistry, 41(7): 706–718.

Bai, Y., Azamdzhon, M., Wang, S., Fang, X., Guo, H., Zhou, P., Chen, C., Liu, X., Jia, S., and Wang, Q., 2019. An evaluation of biological and climatic effects on plant n-alkane distributions and δ^2H_{alk} in a field experiment conducted in central Tibet. Organic Geochemistry, 135: 53–63.

Bird, B.W., Polisar, P.J., Lei, Y.B., Thompson, L.G., Yao, T.D., Finney, B.P., Bain, D.J., Pompeani, D.P., and Steinman, B.A., 2014. A Tibetan lake sediment record of Holocene Indian summer monsoon variability. Earth and Planetary Science Letters, 399: 92–102.

Blaauw, M., and Christen, J.A., 2011. Flexible paleoclimate age-depth models using an autoregressive gamma process. Bayesian Analysis, 6(3): 457–474.

Brown, E.T., Bendick, R., Bourles, D.L., Gaur, V., Molnar, P., Raisbeck, G.M., and Yiou, F., 2003. Early Holocene climate recorded in geomorphological features in Western Tibet. Palaeogeography Palaeoclimatology, Palaeoecology, 199(1–2): 141–151.

Bush, R.T., and McInerney, F.A., 2015. Influence of temperature and C_4 abundance on *n*-alkane chain length distributions across the central USA. Organic Geochemistry, 79: 65–73.

Callegaro, A., Battistel, D., Kehrwald, N.M., Matsubara Pereira, F., Kirchgeorg, T., Villoslada Hidalgo, M.D.C., Bird, B.W., and Barbante, C., 2018. Fire, vegetation, and Holocene climate in a southeastern Tibetan lake: a multi-biomarker reconstruction from Paru Co. Climate of the Past, 14(10): 1543–1563.

Chen, J.A., Wan, G., Zhang, D.D., Zhang, F., and Huang, R., 2004. Environmental records of lacustrine sediments in different time scales: Sediment grain size as an example. Science in China Series D: Earth Sciences, 47(10): 954–960.

Chu, G., Sun, Q., Xie, M., Lin, Y., Shang, W., Zhu, Q., Shan, Y., Xu, D., Rioual, P., Wang, L., and Liu, J., 2014. Holocene cyclic climatic variations and the role of the Pacific Ocean as recorded in varved sediments from northeastern China. Quaternary Science Reviews, 102: 85–95.

Diefendorf, A.F., and Freimuth, E.J., 2017. Extracting the most from terrestrial plant-derived *n*-alkyl lipids and their carbon isotopes from the sedimentary record, A review. Organic Geochemistry, 103: 1–21.

Dietze, E., Maussion, F., Ahlborn, M., Diekmann, B., Hartmann, K., Henkel, K., Kasper, T., Lockot, G., Opitz, S., and Haberzettl, T., 2014. Sediment transport processes across the Tibetan Plateau inferred from robust grain-size end members in lake sediments. Climate of the Past, 10(1): 91–106.

Duan, Y., and Xu, L., 2012. Distributions of *n*-alkanes and their hydrogen isotopic composition in plants from Lake Qinghai (China) and the surrounding area. Applied Geochemistry, 27 (3): 806–814.

Duarte, C. M. and Kalff, J., 1986. Littoral slope as a predictor of the maximum biomass of submerged macrophyte communities. Limnology and Oceanography, 31(5): 1072–1080.

Eley, Y.L., and Hren, M.T., 2018. Reconstructing vapor pressure deficit from leaf wax lipid molecular distributions.Scientific Reports, 8(1): 3967.

Fan, H., Gasse, F., Huc, A., Li, Y., Sifeddine, A., and Soulié-Märsche, I., 1996. Holocene environmental changes in Bangong Co basin (Western Tibet). Part 3: Biogenic remains, Palaeogeography, Palaeoclimatology, Palaeoecology, 120(1-2): 65–78.

Ficken, K.J., Li, B., Swain, D.L., and Eglinton, G., 2000. An *n*-alkane proxy for the sedimentary input of submerged/floating freshwater aquatic macrophytes. Organic Geochemistry, 31 (7): 745–749.

Fontes, J.-C., Gasse, F., and Gibert, E., 1996. Holocene environmental changes in Lake Bangong basin (Western Tibet). Part 1: Chronology and stable isotopes of carbonates of a Holocene lacustrine core. Palaeogeography, Palaeoclimatology, Palaeoecology, 120(1–2): 25–47.

Freeman, K.H., and Pancost, R.D., 2014. 12.15 - Biomarkers for Terrestrial Plants and Climate. In: Holland, H.D., and Turekian, K.K. (eds.), Treatise on Geochemistry (Second Edition), Elsevier, Oxford.

Gao, L., Hou, J., Toney, J., MacDonald, D., and Huang, Y., 2011. Mathematical modeling of the aquatic macrophyte inputs of mid-chain *n*-alkyl lipids to lake sediments: Implications for interpreting compound specific hydrogen isotopic records. Geochimica et Cosmochimica Acta, 75(13): 3781–3791.

Gasse, F., Arnold, M., Fontes, J.C., Fort, M., Gibert, E., Huc, A., Li, B.Y., Li, Y.F., Lju, Q., Melieres, F., Vancampo, E., Wang, F.B., and Zhang, Q.S., 1991. A 13,000-year climate Record from Western Tibet. Nature, 353(6346): 742–745.

Gasse, F., Fontes, J.C., Van Campo, E., and Wei, K., 1996. Holocene environmental changes in Bangong Co basin (Western Tibet). Part 4: Discussion and conclusions. Palaeogeography, Palaeoclimatology, Palaeoecology, 120(1–2): 79–92.

Gasse, F., and Van Campo, E., 1994. Abrupt post-glacial climate events in West Asia and North Africa monsoon domains. Earth and Planetary Science Letters, 126(4): 435–456.

Guenther, F., Aichner, B., Siegwolf, R., Xu, B.Q., Yao, T.D., and Gleixner, G., 2013. A synthesis of hydrogen isotope variability and its hydrological significance at the Qinghai-Tibetan Plateau. Quaternary International, 313–314: 3–16.

Günther, F., Thiele, A., Biskop, S., Mäusbacher, R., Haberzettl, T., Yao, T., and Gleixner, G., 2016. Late quaternary hydrological changes at Tangra Yumco, Tibetan Plateau: a compound-specific isotope-based quantification of lake level changes. Journal of Paleolimnology, 55(4): 369–382.

Günther, F., Witt, R., Schouten, S., Mäusbacher, R., Daut, G., Zhu, L., Xu, B., Yao, T., and Gleixner, G., 2015. Quaternary ecological responses and impacts of the Indian Ocean Summer Monsoon at Nam Co, Southern Tibetan Plateau. Quaternary Science Reviews, 112: 66–77.

Guo, Y., Guo, N., He, Y., and Gao, J., 2015. Cuticular waxes in alpine meadow plants: climate effect inferred from latitude gradient in Qinghai-Tibetan Plateau. Ecology and Evolution, 5 (18): 3954–3968.

He, Y., Zheng, Y., Pan, A., Zhao, C., Sun, Y., Song, M., Zheng, Z., and Liu, Z., 2014. Biomarker-based reconstructions of Holocene lake-level changes at Lake Gahai on the northeastern Tibetan Plateau. The Holocene, 24(4): 405–412.

Hou, J., D'Andrea, W.J., Wang, M., He, Y., and Liang, J., 2017. Influence of the Indian monsoon and the subtropical jet on climate change on the Tibetan Plateau since the late Pleistocene. Quaternary Science Reviews, 163: 84-94.

Hou, J., D’Andrea, W.J., and Huang, Y., 2008. Can sedimentary leaf waxes record D/H ratios of continental precipitation? Field, model, and experimental assessments. Geochimica et Cosmochimica Acta, 72(14): 3503–3517.

Hou, J., Tian, Q., and Wang, M., 2018. Variable apparent hydrogen isotopic fractionation between sedimentary *n*-alkanes and precipitation on the Tibetan Plateau. Organic Geochemistry, 122: 78–86.

Hou, J.Z., Huang, Y.S., Zhao, J.T., Liu, Z.H., Colman, S., and An, Z.S., 2016. Large Holocene summer temperature oscillations and impact on the peopling of the northeastern Tibetan Plateau. Geophysical Research Letters, 43(3): 1323–1330.

Hu, X., Zhu, L., Wang, Y., Wang, J., Peng, P., Ma, Q., Hu, J., and Lin, X., 2014. Climatic significance of *n*-alkanes and their compound-specific δD values from lake surface sediments on the Southwestern Tibetan Plateau. Chinese Science Bulletin, 59(24): 3022–3033.

Jia, Q., Sun, Q., Xie, M., Shan, Y., Ling, Y., Zhu, Q., and Tian, M., 2016. Normal alkane distributions in soil samples along a Lhasa-Bharatpur Transect. Acta Geologica Sinica (English Edition), 90(2): 738–48.

Jin, C., Günther, F., Li, S., Jia, G., Peng, P.A., and Gleixner, G., 2015. Reduced early Holocene moisture availability inferred from δD values of sedimentary *n*-alkanes in Zigetang Co, Central Tibetan Plateau. The Holocene, 26(4): 556–566.

Khan, A., Richards, K.S., Parker, G.T., McRobie, A., and Mukhopadhyay, B., 2014. How large is the Upper Indus Basin? The pitfalls of auto-delineation using DEMs. Journal of Hydrology, 509: 442–453.

Kong, P., Na, C., Fink, D., Huang, F., and Ding, L., 2007: Cosmogenic ^{10}Be inferred lake-level changes in Sumxi Co basin, Western Tibet. Journal of Asian Earth Sciences, 29(5–6), 698–703.

Lei, Y., Yang, K., Wang, B., Sheng, Y., Bird, B.W., Zhang, G., and Tian, L., 2014. Response of inland lake dynamics over the Tibetan Plateau to climate change. Climatic Change, 125(2): 281–290.

Leipe, C., Demske, D., Tarasov, P.E., and Members, H.P., 2014. A Holocene pollen record from the northwestern Himalayan lake Tso Moriri: Implications for palaeoclimatic and archaeological research. Quaternary International, 348: 93–112.

Li, X., Wang, M., Zhang, Y., Lei, L., and Hou, J., 2017. Holocene climatic and environmental change on the western Tibetan Plateau revealed by glycerol dialkyl glycerol tetraethers and leaf wax deuterium-to-hydrogen ratios at Aweng Co. Quaternary Research, 87(3): 455–467.

Lin, X., Zhu, L., Wang, Y., Wang, J., Xie, M., Ju, J., Mäusbacher, R., and Schwalb, A., 2008. Environmental changes reflected by *n*-alkanes of lake core in Nam Co on the Tibetan Plateau since 8.4 kaB.P. Chinese Science Bulletin, 53(19): 3051–3057.

Ling, Y., Sun, Q., Zheng, M., Wang, H., Luo, Y., Dai, X., Xie, M., and Zhu, Q., 2017a. Alkenone-based temperature and climate reconstruction during the last deglaciation at Lake Dangxiong Co, southwestern Tibetan Plateau, Quaternary International, 443: 58–69.

Ling, Y., Zheng, M., Sun, Q., and Dai, X., 2017b. Last deglacial climatic variability in Tibetan Plateau as inferred from *n*-alkanes in a sediment core from Lake Zabuye, Quaternary International, 454: 15–24.

Ling, Y., Zheng, M., Xie, B., Wang, S., Sun, Q., Zhang, Y., and Zhang, C. The Impact of Climatic and Environmental Factors on *n*-Alkanes Indices in Southwestern Tibetan Plateau. Acta Geologica Sinica (English Edition), doi: 10.1111/1755-6724.14376.

Liu, H., and Liu, W., 2016. *n*-Alkane distributions and concentrations in algae, submerged plants and terrestrial plants from the Qinghai-Tibetan Plateau. Organic Geochemistry, 99: 10–22.

Liu, W., Liu, H., Wang, Z., An, Z., and Cao, Y., 2017. Hydrogen isotopic compositions of long-chain leaf wax *n*-alkanes in Lake Qinghai sediments record palaeohydrological variations during the past 12 ka. Quaternary International, 449: 67–74.

Liu, W.G., Yang, H., Wang, H. Y., An, Z. S., Wang, Z., and Leng, Q., 2015: Carbon isotope composition of long chain leaf wax *n*-alkanes in lake sediments: A dual indicator of paleoenvironment in the Qinghai-Tibet Plateau. Organic Geochemistry, 83-84: 190–201.

Liu, Y.W., Xu-Ri, Wang, Y.S., Pan, Y.P., and Piao, S.L., 2015. Wet deposition of atmospheric inorganic nitrogen at five remote sites in the Tibetan Plateau. Atmospheric Chemistry and Physics, 15(20):11683-11700.

Macumber, A.L., Patterson, R.T., Galloway, J.M., Falck, H., and Swindles, G.T., 2018. Reconstruction of Holocene hydroclimatic variability in subarctic treeline lakes using lake sediment grain-size end-members. The Holocene, 28(6): 845–857.

Middelboe, A.L., and Markager, S., 1997. Depth limits and minimum light requirements of freshwater macrophytes. Freshwater Biology, 37(3): 553–568.

Mischke, S., Weynell, M., Zhang, C.J., and Wiechert, U., 2013. Spatial variability of ^{14}C reservoir effects in Tibetan Plateau lakes. Quaternary International, 313-314: 147–155.

Mügler, I., Sachse, D., Werner, M., Xu, B., Wu, G., Yao, T., and Gleixner, G., 2008. Effect of lake evaporation on δD values of lacustrine *n*-alkanes: A comparison of Nam Co (Tibetan Plateau) and Holzmaar (Germany). Organic Geochemistry, 39 (6): 711–729.

Peng, Y., Xiao, J., Nakamura, T., Liu, B., and Inouchi, Y., 2005. Holocene East Asian monsoonal precipitation pattern revealed by grain-size distribution of core sediments of Daihai Lake in Inner Mongolia of north-central China. Earth and Planetary Science Letters, 233(3): 467–479.

Poynter, J., and Eglinton, G., 1990. 14. Molecular composition of three sediments from hole 717C: The Bengal Fan. Proceeding of the Ocean Drilling Program, Scientific Results, 116:155–161.

Poynter, J.G., Farrimond, P., Robinson, N., and Eglinton, G., 1989. Aeolian-derived higher plant lipids in the marine sedimentary record: Links with palaeoclimate. In: Leinen, M., and Sarnthein, M. (eds.), Paleoclimatology and Paleometeorology: Modern and Past Patterns of Global Atmospheric Transport, Springer Netherlands, Dordrecht.

Pu, Y., Nace, T., Meyers, P.A., Zhang, H., Wang, Y., Zhang, C.L., and Shao, X., 2013. Paleoclimate changes of the last 1000 yr on the eastern Qinghai–Tibetan Plateau recorded by elemental, isotopic, and molecular organic matter proxies in sediment from glacial Lake Ximencuo, Palaeogeography, Palaeoclimatology, Palaeoecology, 379–380: 39–53.

Pu, Y., Zhang, H., Wang, Y., Lei, G., Nace, T., and Zhang, S., 2011. Climatic and environmental implications from *n*-alkanes in glacially eroded lake sediments in Tibetan Plateau: An example from Ximen Co. Chinese Science Bulletin, 56(14): 1503.

Qiao, B., and Zhu, L., 2019. Difference and cause analysis of water storage changes for glacier-fed and non-glacier-fed lakes on the Tibetan Plateau. Science of The Total Environment, 693: 133399.

Sachse, D., Billault, I., Bowen, G.J., Chikaraishi, Y., Dawson, T.E., Feakins, S.J., Freeman, K.H., Magill, C.R., McInerney, F.A., van der Meer, M.T.J., Polissar, P., Robins, R.J., Sachs, J.P., Schmidt, H.L., Sessions, A.L., White, J.W.C., West, J.B., and Kahmen, A., 2012. Molecular paleohydrology: Interpreting the hydrogen-isotopic composition of lipid biomarkers from photosynthesizing organisms. Annual Review of Earth and Planetary Sciences, 40(1): 221–249.

Saini, J., Gunther, F., Aichner, B., Mischke, S., Herzschuh, U., Zhang, C.J., Mausbacher, R., and Gleixner, G., 2017. Climate variability in the past similar to 19,000 yr in NE Tibetan Plateau inferred from biomarker and stable isotope records of Lake Donggi Cona. Quaternary Science Reviews, 157: 129–140.

Schefuß, E., Ratmeyer, V., Stuut, J.-B. W., Jansen, J.H.F., and Sinninghe Damsté, J.S., 2003. Carbon isotope analyses of *n*-alkanes in dust from the lower atmosphere over the central eastern Atlantic. Geochimica et Cosmochimica Acta, 67(10): 1757–1767.

Shi, Y., Kong, Z., Wang, S., Tang, L., Wang, F., Yao, T., Zhao, X., Zhang, P., and Shi, S., 1993. Mid-Holocene climates and environments in China. Global and Planetary Change, 7(1–3): 219–233.

Shi, Y.F., Yu, G., Liu, X.D., Li, B.Y., and Yao, T.D., 2001. Reconstruction of the 30-40 ka BP enhanced Indian monsoon climate based on geological records from the Tibetan Plateau. Palaeogeography Palaeoclimatology Palaeoecology, 169(1–2): 69–83.

Sun, H., Bendle, J., Seki, O., and Zhou, A., 2018. Mid- to- late Holocene hydroclimatic changes on the Chinese Loess Plateau: evidence from *n*-alkanes from the sediments of Tianchi Lake. Journal of Paleolimnology, 60(4): 511–523.

Taft, L., Wiechert, U., Albrecht, C., Leipe, C., Tsukamoto, S., Wilke, T., Zhang, H., and Riedel, F., 2020. Intra-seasonal hydrological processes on the western Tibetan Plateau: Monsoonal and convective rainfall events at ~7.5 ka. Quaternary International, 537: 9–23.

Thompson, L.G., Yao, T., Davis, M.E., Henderson, K.A., MosleyThompson, E., Lin, P.N., Beer, J., Synal, H.A., ColeDai, J., and Bolzan, J.F., 1997. Tropical climate instability: The last glacial cycle from a Qinghai-Tibetan ice core. Science, 276(5320): 1821–1825.

Wan, W., Long, D., Hong, Y., Ma, Y., Yuan, Y., Xiao, P., Duan, H., Han, Z., and Gu, X., 2016. A lake data set for the Tibetan Plateau from the 1960s, 2005, and 2014, Scientific Data, 3: 160039.

Wang, G., Wang, Y., Wei, Z., He, W., Ma, X., Sun, Z., Xu, L., Gong, J., Wang, Z., and Pan, Y., 2019. Paleoclimate changes of the past 30 cal ka BP inferred from lipid biomarkers and geochemical records from Qionghai Lake, southwest China. Journal of Asian Earth Sciences, 172: 346–358.

Wang, J., Axia, E., Xu, Y., Wang, G., Zhou, L., Jia, Y., Chen, Z., and Li, J., 2018. Temperature effect on abundance and distribution of leaf wax *n*-alkanes across a temperature gradient along the 400 mm isohyet in China. Organic Geochemistry, 120: 31–41.

Wang, M.D., Hou, J.Z., and Lei, Y.B., 2014. Classification of Tibetan lakes based on variations in seasonal lake water temperature. Chinese Science Bulletin, 59: 4847–4855.

Wang, Y.B., Herzschuh, U., Shumilovskikh, L.S., Mischke, S., Birks, H.J.B., Wischnewski, J., Böhner, J., Schlütz, F., Lehmkuhl, F., Diekmann, B., Wünnemann, B., and Zhang, C., 2014. Quantitative reconstruction of precipitation changes on the NE Tibetan Plateau since the Last Glacial Maximum - extending the concept of pollen source area to pollen-based climate reconstructions from large lakes. Climate of the Past, 10(1): 21–39.

Wang, Y., Wang, J., Zhu, L., Lin, X., Hu, J., Ma, Q., Ju, J., Peng, P., and Yang, R., 2017. Mid- to late-Holocene paleoenvironmental changes inferred from organic geochemical proxies in Lake Tangra Yumco, Central Tibetan Plateau. The Holocene, 27(10): 1475–1486.

Wang, Y., Zhu, L., Wang, J., Ju, J., Peng, P., Lin, X., Hu, J., and

Nishimura, M., 2016. Paleohydrological processes revealed by *n*-alkane δD in lacustrine sediments of Lake Pumoyum Co, southern Tibetan Plateau, and their response to climate changes during the past 18.5 cal ka. Journal of Paleolimnology, 56(2–3): 223–238.
Wang, Z., Liu, Z.H., Zhang, F., Fu, M.Y., and An, Z.S., 2015. A new approach for reconstructing Holocene temperatures from a multi-species long chain alkenone record from Lake Qinghai on the northeastern Tibetan Plateau. Organic Geochemistry, 88: 50–58.
Wang, Z., Zhang, F., Li, X., Cao, Y., Hu, J., Wang, H., Lu, H., Li, T., and Liu, W., 2020. Changes in the depth of Lake Qinghai since the last deglaciation and asynchrony between lake depth and precipitation over the northeastern Tibetan Plateau. Global and Planetary Change, 188: 103156.
Wen, R., Tian, L.D., Liu, F.J., and Qu, D.M., 2016. Lake water isotope variation linked with the in-lake water cycle of the alpine Bangong Co, arid western Tibetan Plateau, Arctic Antarctic and Alpine Research, 48(3): 563–580.
Witt, R., Gunther, F., Lauterbach, S., Kasper, T., Mausbacher, R., Yao, T.D., and Gleixner, G., 2016. Biogeochemical evidence for freshwater periods during the Last Glacial Maximum recorded in lake sediments from Nam Co, south-central Tibetan Plateau. Journal of Paleolimnology, 55(1): 67–82.
Wünnemann, B., Mischke, S., and Chen, F., 2006. A Holocene sedimentary record from Bosten Lake, China. Palaeogeography, Palaeoclimatology, Palaeoecology, 234(2): 223–238.
Yan, T., He, J., Wang, Z., Zhang, C., Feng, X., Sun, X., Leng, C., and Zhao, C., 2020: Glacial fluctuations over the last 3500 years reconstructed from a lake sediment record in the northern Tibetan Plateau. Palaeogeography, Palaeoclimatology, Palaeoecology, 544: 109597.
Yang, R., Zhu, L., Wang, J., Ju, J., Ma, Q., Turner, F., and Guo, Y., 2017. Spatiotemporal variations in volume of closed lakes on the Tibetan Plateau and their climatic responses from 1976 to 2013. Climatic Change, 140(3): 621–633.
Yao, T., Xue, Y., Chen, D., Chen, F., Thompson, L., Cui, P., Koike, T., Lau, W.K.M., Lettenmaier, D., Mosbrugger, V., Zhang, R., Xu, B., Dozier, J., Gillespie, T., Gu, Y., Kang, S., Piao, S., Sugimoto, S., Ueno, K., Wang, L., Wang, W., Zhang, F., Sheng, Y., Guo, W., Ailikun, Yang, X.X, Ma, Y.M., Shen, S.S.P., Su, Z., Chen, F., Liang, S., Liu, Y., Singh, V.P., Yang, K., Yang, D., Zhao, X., Qian, Y., Zhang, Y., and Li, Q., 2018. Recent third pole's rapid warming accompanies cryospheric melt and water cycle intensification and interactions between monsoon and environment: Multidisciplinary approach with observations, modeling, and analysis. Bulletin of the American Meteorological Society, 100(3): 423–444.
Yao, T.D., Thompson, L., Yang, W., Yu, W.S., Gao, Y., Guo, X.J., Yang, X.X., Duan, K.Q., Zhao, H.B., Xu, B.Q., Pu, J.C., Lu, A.X., Xiang, Y., Kattel, D.B., and Joswiak, D., 2012. Different glacier status with atmospheric circulations in Tibetan Plateau and surroundings. Nature Climate Change, 2(9): 663–667.
Zhang, G., Xie, H., Kang, S., Yi, D., and Ackley, S. F., 2011. Monitoring lake level changes on the Tibetan Plateau using ICESat altimetry data (2003–2009). Remote Sensing of Environment, 115(7): 1733–1742.
Zhang, X., Xu, B., Günther, F., Witt, R., Wang, M., Xie, Y., Zhao, H., Li, J., and Gleixner, G., 2017. Rapid northward shift of the Indian Monsoon on the Tibetan Plateau at the end of the Little Ice Age. Journal of Geophysical Research: Atmospheres, 122(17): 9262–9279.
Zhao, C., Liu, Z.H., Rohling, E.J., Yu, Z.C., Liu, W.G., He, Y.X., Zhao, Y., and Chen, F.H., 2013. Holocene temperature fluctuations in the northern Tibetan Plateau. Quaternary Research, 80(1): 55–65.
Zhao, J., An, C.-B., Huang, Y., Morrill, C., and Chen, F.-H., 2017. Contrasting early Holocene temperature variations between monsoonal East Asia and westerly dominated Central Asia. Quaternary Science Reviews, 178: 14–23.

About the first author

WANG Mingda, male, born in 1983 in Shenyang City, Liaoning Province; graduated from the University of Chinese Academy of Sciences; Postdoctoral researcher at the Institute of Tibetan Plateau Research, Chinese Academy of Sciences. He is interested in organic molecules, called 'biomarkers', to understand how climate change impacted the world in the past. Email: mdwang@itpcas.ac.cn; phone: 18600498031. Current address: School of Geography, Liaoning Normal University, Dalian 116029, Liaoning.

About the corresponding author

HOU Juzhi, male, born in 1975 in Xingtai City, Hebei Province; he received his Ph.D. degrees in 2003 from the Institute of Geology and Geophysics, CAS, and in 2008 from Brown University; research professor at the Institute of Tibetan Plateau Research, Chinese Academy of Sciences (CAS) and CAS Center for Excellence in Tibetan Plateau Earth Sciences. His research topic is quantitative reconstruction of Holocene temperature and precipitation on the Tibetan Plateau using biomarkers. Email: houjz@itpcas.ac.cn; phone: 010-84097077.